What determines the critical size for phase separation in $LiFePO_4$ in lithium ion batteries?

Tetsu Ichitsubo,[a]* Takayuki Doi,[b]† Kazuya Tokuda,[a] Eiichiro Matsubara,[a]
Tetsuya Kida,[c] Tomoya Kawaguchi,[a] Shunsuke Yagi,[d] Shigeto Okada,[e] Jun-ichi Yamaki[e]

[a] *Department of Materials Science and Engineering, Kyoto University, Kyoto 606-8501, Japan*
[b] *Department of Molecular Chemistry and Biochemistry, Doshisha University, Kyotanabe, Kyoto 610-0321, Japan*
[c] *Department of Energy and Material Sciences, Kyushu University, Kasuga 816-8580, Japan*
[d] *Nanoscience and Nanotechnology Research Center, Osaka Prefecture University, Osaka 599-8570, Japan*
[e] *Institute for Materials Chemistry and Engineering, Kyushu University, Kasuga 816-8580, Japan*

(Dated: September 17, 2013)

$LiFePO_4$ characteristically shows a plateau voltage due to a two-phase ($LiFePO_4$/$FePO_4$) separation during charge/discharge process in Li ion batteries. In this study, we clearly show that monodispersed nano-sized (about 10 nm) $LiFePO_4$ particles exhibit a complete single-phase reaction without showing any plateau voltage. Since the elastic strain due to lattice mismatch between $LiFePO_4$ and $FePO_4$ would be easily released near the surface, elastic effects are usually expected to be weaken as the particle size, but, in contrast to this expectation, phase separation does not occur experimentally in such small nanoparticles. Consideration on the basis only of static thermodynamics is insufficient to explain why such a single-phase reaction occurs in nano-sized particles. Contrary, the mechanism of the single-phase reaction can naturally be understood, when we consider a kinetics concept based on the preferred wavelength for stable growth of the spinodal wave under such an elastic constraint.

1. INTRODUCTION

Lithium ion batteries (LIBs) are seeing widespread use in large-sized applications such as automobiles, which raises expectations for storage batteries with a higher performance, combined with renewable energy technologies, to realize a sustainable society. The performance of LIBs, with regard to energy density, rate capability, cyclability and safety, has been steadily improved since their launch in 1991. Since LIBs are simply based on the transfer of Li ion between the negative and positive electrodes, the electromotive force of LIBs depends on the difference in the chemical potential of Li atoms between the two electrodes.

Due to its fascinating fast charge/discharge properties, $LiFePO_4$ has attracted increasing attention for the use in practical battery applications. Electrochemical Li ion insertion and extraction reactions at $LiFePO_4$ take place at around ca. 3.4 V with high reversibility. However, $LiFePO_4$ has the intrinsically low electronic conductivity (10^{-9}-10^{-11} S cm^{-1}). In fact, only 70 % of Li can be extracted from $LiFePO_4$ even at low-rate discharge conditions (0.05 mA cm^{-2}), which was reported in the pioneering work by Goodenough et al.[1] in 1997. Afterward several effective ways have been proposed to overcome this drawback; (1) Carbon-coating of $LiFePO_4$ enhanced the conductivity of the positive electrode.[2] (2) Selective doping with supervalent cations increased the bulk electronic conductivity.[3] (3) The use of very fine particles of $LiFePO_4$ shortened both the conduction path of electrons and the diffusion path of Li ion, which resulted in the improvement of the rate capability of $LiFePO_4$.[4] However, the optimum particle size has not been revealed yet; the effects of the particle size of $LiFePO_4$ on the electrode performance have been less well understood. In general, $LiFePO_4$ shows a constant working electrode potential of 3.42 V, which suggests that the insertion/extraction reactions of Li ion basically proceed by varying the volume (mole) fraction of $LiFePO_4$/$FePO_4$ in the two-phase equilibrium.

However, Yamada et al.[5] clearly showed that there are two solid-solution regions outside the endpoints of the miscibility gap at room temperature. The miscibility gap shrinks and solid-solution regions extend with a reduced size of $LiFePO_4$ particles.[6–8] Gibot et al.[9] prepared nano-sized particles (including crystalline disorder) about 40 nm in diameter, and demonstrated by X-ray diffraction that insertion and extraction reactions of Li ion proceeded along with the formation of a solid solution of Li_xFePO_4 over almost the entire composition region, while a voltage

* Email: tichi@mtl.kyoto-u.ac.jp
† Email: tdoi@mail.doshisha.ac.jp

plateau at around 3.42 V was still observed, which suggested the mixing of coarse particles. Thus, the use of nanotechnology could not only greatly improve the charge and discharge performance of $LiFePO_4$, but it could also lead to the disappearance of a phase separation, that is, monodispersed nano-sized $LiFePO_4$ particles may realize facile charge/discharge performance due to a phase-separation-free process.

On the other hand, many recent reports have indicated that phase separation kinetics are significantly suppressed and retarded.[10–12] These interesting phenomena are generally believed to be due to elastic strain caused by lattice mismatch,[8, 13] and discussion on the strain is thought to become gradually activated. Although the previous computer-simulation studies[14, 15] have fairly clarified the effects of the coherent elastic strain on the phase-separation kinetics and microstructure formation, it is not yet clarified how the elastic strain affects the phase separation on very small particles less than 40 nm in diameter. Intuitively, in terms of the elastic strain energy, smaller particles usually have the advantage of a prompt phase transition due to the surface effect, whereby the elastic strain is easily released near the surface, and the surface effects are enhanced as the particle size decreases. It would be interesting to determine what would happen with a further decrease in the particle size of monodispersed $LiFePO_4$. Here, we experimentally show for the first time that nanocrystals of $LiFePO_4$ with a uniform size of about 10 nm are charged and discharged in a "complete single-phase state". Subsequently, on the basis of Cahn's spinodal decomposition theory,[16–18] we present a significant conclusion regarding the critical size for "phase-separation-free" particles.

2. EXPERIMENTAL

2.1. Fabrication procedure

A mixture of 1 mmol oleic acid, 33.8 mmol oleylamine, 1 mmol phosphoric acid, 1 mmol lithium hydroxide monohydrate and 1 mmol iron was heated to 280°C at 10°C/min, and kept at that temperature for 3 h under an Ar atmosphere. The synthesis temperature and holding time are key factors in the synthesis of uniformly-small-sized particles; these conditions, as well as the atmospheric control, have an especially-strong influence on the particle size of $LiFePO_4$. The resultant solution was poured into an excess amount of ethanol, and the mixture was centrifuged to obtain deposits. The deposits were washed several times in a mixture of ethanol and hexane. The products were characterized by X-ray diffraction (XRD), and typical working conditions were 50 kV and 300 mA at a scanning speed of 0.25°/min. The resultant particles were dispersed in hexane, and then dropped on carbon-coated copper grids so that their morphology could be observed by transmission electron microscopy (TEM).

The charge and discharge properties were investigated using a coin-type cell. The test electrode was composed of the resultant particles (70 wt%), acetylene black (25 wt%), and poly(vinylidene fluoride) (5 wt%). Li foil and polypropylene film were used as the counter electrode and separator, respectively. The electrolyte used was 1 mol/dm^3 $LiPF_6$ dissolved in a mixture of ethylene carbonate (EC) and dimethyl carbonate (DMC) (1:1, v/v). The charge/discharge cycles were carried out at a constant current rate of 0.01 C, which corresponds to the current density (1.71 mA/g) so that each charge and discharge process should theoretically be completed in 100 hours. The charge and discharge processes ended at 4.0 V and 2.0 V, respectively. Cell assembly was conducted under an Ar atmosphere with a dew point below −70°C.

2.2. Structure of nano-sized particles and their electrochemical properties

Figure 1(a) shows XRD patterns of the resultant particles, in which all of the diffraction peaks are identified as phospho-olivine $LiFePO_4$; a very small peak was observed at around 23.2°, which is identified as Li_3PO_4. Figure 1(b) shows typical TEM image of $LiFePO_4$ particles; fairly uniform particles with distinct crystal forms were observed. The particle diameter was about 10 nm, as well as in the previous report.[19] Figure 1(c) shows charge (extraction of Li ion from $LiFePO_4$) and discharge (insertion of Li ion into $FePO_4$) curves obtained at a very slow rate of 0.01 C. The discharge capacity was evaluated to be 68 mAh/g, which was much smaller than the theoretical capacity of 170 mAh/g even though the charge/discharge rates were relatively slow. The most distinct feature in Fig. 1(c) was that charge/discharge curves sloped without any plateau region. This behavior was quite different from those observed for micron-sized $LiFePO_4$ powder: insertion and extraction reactions of Li ion at $LiFePO_4$ usually take place at about 3.42 V under a two-phase equilibrium, and hence a clear plateau is seen at that voltage in charge/discharge curves.

As mentioned above, extraction/insertion reactions of Li ions for nanoparticles of about 40 nm proceed with retention of a solid solution of Li_xFePO_4 in terms of X-ray diffraction, but the voltage plateaus at around 3.42 V (in addition to sloping voltage curves) were still observed in the charge/discharge curves.[7, 9] On the other hand, the

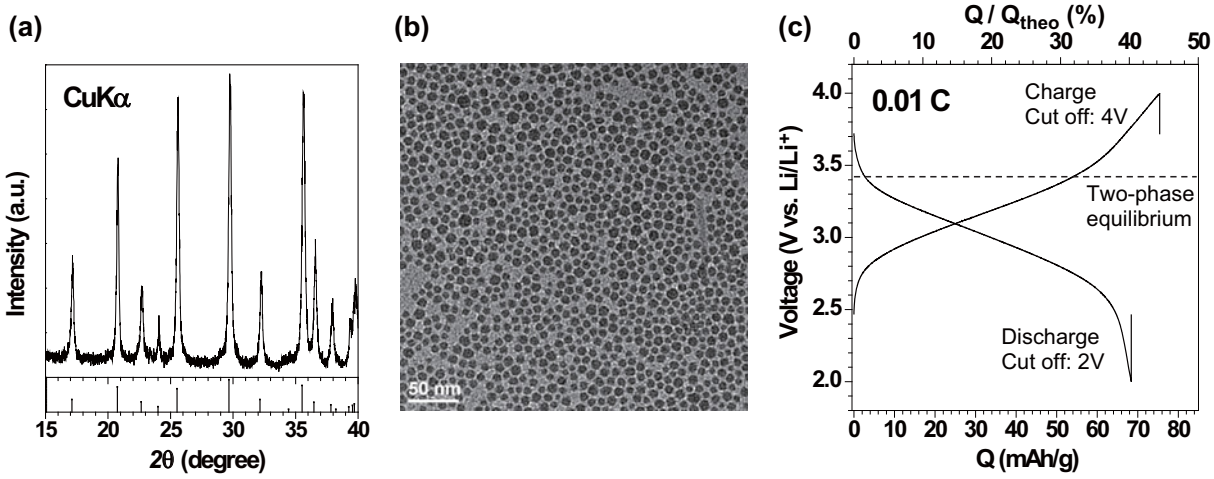

FIG. 1: Experimental observation of single-phase reaction for monodispersed nano-sized $LiFePO_4$ particles prepared at 280°C. (a) X-ray diffraction profile with a powder diffraction file (PDF #40-1499), (b) TEM image, and (c) charge and discharge curves at a slow C rate of 0.01C, where $Q/Q_{\rm theo}$ denotes the ratio of the capacity Q to the theoretical capacity.

$LiFePO_4$ nanocrystals used here were very small (about 10 nm) and fairly uniform; in this case, the average potentials of the charge and discharge reactions were as low as 3.3 and 3.0 V, respectively, which were both lower than the typical working potential of 3.42 V, and is a peculiar feature of nano-sized $LiFePO_4$. Thus, when monodispersed particles are about 10 nm in diameter, the charge/discharge curves are those of a single-phase reaction, and obviously not those of a conventional two-phase equilibrium.

3. ON THE MISCIBILITY GAP

3.1. Effects of elastic strain energy

In order to understand the single-phase reaction of $LiFePO_4$ nanoparticles, first of all, we have to consider the miscibility gap of the $LiFePO_4/FePO_4$ system by taking into account the elastic-strain energy caused by the lattice mismatch and the interfacial energy brought by the phase separation. We here employ the two kinds of treatments; one is based on static thermodynamics and the other is based on the kinetics theory.

First we shall consider the effects of strain energy on the phase separation based on static thermodynamics. In our recent paper,[15] we revealed that nucleation in this system is unlikely to occur on the interior of the active materials; nucleation, if any, can take place only near the surface where the elastic strain can be easily released. Consequently, the system would remain in a single phase until the overall Li composition reaches the spinodal decomposition region, resulting in the suppression of the phase decomposition of the system, as discussed in recent papers.[13, 14]

To understand the influence of elastic strain on spinodal decomposition, we consider a typical case in which spinodal decomposition occurs at $\phi = 0.5$ (i.e., $c_{\rm Li} = 0.5$) in the symmetric free energy of a regular solution type,

$$f(\phi) = \Omega\phi(1-\phi) + RT\left[\phi\ln\phi + (1-\phi)\ln(1-\phi)\right], \tag{1}$$

where R is the gas constant, T is the absolute temperature, Ω is the interaction parameter of the regular solution. ϕ is defined as $\phi = 1 - c_{\rm Li}$, where $c_{\rm Li}$ is the Li composition at the lithium site of the olivine structure, i.e., ϕ is the Li-vacancy (denoted as V_{Li}) composition. According to the literature, [14, 20] the value of Ω is about 12 kJ/mol for the $LiFePO_4/FePO_4$ system. When we consider the free-energy density function per unit volume, Eq. (1) has to be divided by the molar volume $V_{\rm m} \approx 43.8 \times 10^{-6}$ m^3/mol. As suggested by Malik et al.,[21] the free energies of two phases may not be so simple, but several works have successfully explained the experimental results in this system by using the free energy of the regular solution type.[22, 23]

In this case, unlike the nucleation process, the lattice mismatch gradually increases with a continuous phase separation; the elastic strain due to the mismatch is given by $T_{mn}(2\phi - 1)/2$ when the two separated phases have ϕ and $1 - \phi$, respectively, where the eigenstrain, $\varepsilon^*_{mn}(\phi)$, by measuring from the lattice constants of $LiFePO_4$, is given by

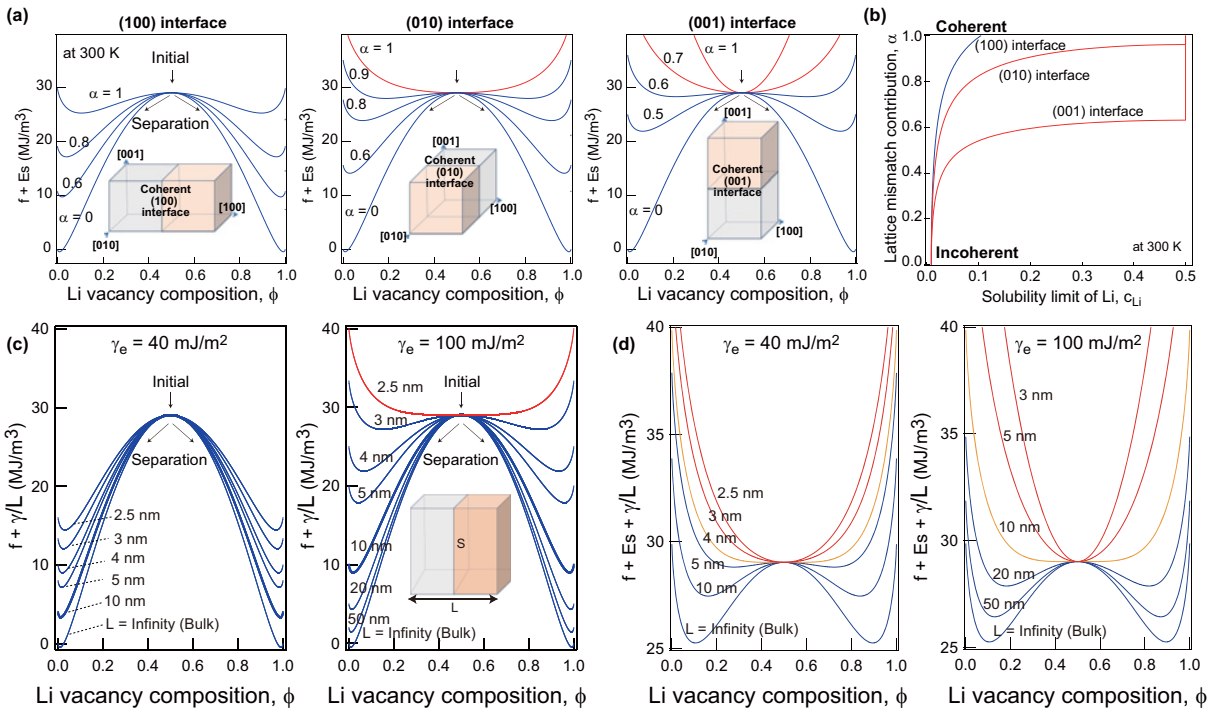

FIG. 2: (a) Sum of the free energy and elastic energy when the phase separation is supposed to occur from $\phi = 0.5$, $f + E_s$, as a function of ϕ for three coherent interfaces corresponding to the illustrations shown in the insets. (b) The solubility limit of Li atoms (lateral axis) as a function of the coherency factor α (vertical axis), determined according to the axes in the phase diagram; $\alpha = 1$ means complete coherency, while $\alpha = 0$ indicates complete incoherency (loss of coherency). (c) Sum of the free energy and interfacial energy, $f + \gamma/L$, as a function of ϕ for $\gamma_e = 40$ and 100 mJ/m^2, when phase separation is supposed to occur from $\phi = 0.5$. (d) The total free energy, $f + E_s + \gamma/L$, as a function of ϕ for $\gamma_e = 40$ and 100 mJ/m^2, where the (100) interface is assumed for the calculation.

$T^*_{11} = -0.050$, $T^*_{22} = -0.036$, $T^*_{33} = 0.019$, and $T^*_{ij} = 0$ for $i \neq j$. If we do not consider microstructural optimization, the elastic energy $E_s(\phi)$ caused by the separation can be given by

$$E_s(\phi) = \frac{1}{2}(c_{1111}T^{*\,2}_{11} + c_{2222}T^{*\,2}_{22} + c_{3333}T^{*\,2}_{33} + 2c_{2233}T^*_{22}T^*_{33} + 2c_{3311}T^*_{33}T^*_{11} + 2c_{1122}T^*_{11}T^*_{22})\left(\frac{1-2\phi}{2}\alpha\right)^2, \quad (2)$$

where α is the coherency factor (contribution factor) of the lattice mismatch, and all components of the 4th-rank elastic constants c_{ijkl} are given by the first-principle calculation (GGA + U);[24] when $\alpha = 1$ the lattice mismatch completely affects the total free energy, while $\alpha = 0$ means a state of complete incoherency.

Based on our previous calculation results,[15] we consider here three simple types of interfaces, (100), (010) and (001) interfaces, as shown in Fig. 2. When the coherent interface caused by spinodal decomposition is normal to the crystallographic [100] axis [called the "(100) interface" or "bc interface"], we can consider $T^*_{11} = 0$, since the [100] direction is free from lattice coherency. Similarly, $T^*_{22} = 0$ for the (010) interface, and $T^*_{33} = 0$ for the (001) interface; e.g., $E_s^{(100)} \approx 4 \times 29.9(\phi - 1/2)^2$ MJ/m^3 for the (100) interface.

Figure 2(a) shows the sum of the free energy and elastic energy, $f+E_s$, for the three coherent interfaces corresponding to the illustrations in the insets. As is clearly shown in the figure, among the three interfaces, only the (100) interface is stable, and the other coherent interfaces are elastically unstable, which is consistent with the experimental observation.[25] The (010) interface can be stable with a slight loss of coherency, but the (001) interface cannot be formed unless the coherent misfit strain is sufficiently released (by misfit dislocations, increase in mosaicity, etc). This trend can be attributed to the ease of release of the eigenstrain;[15] in this olivine case, the lattice mismatch along the a axis is largest between the $LiFePO_4$ and $FePO_4$ phases.

Figure 2(b) shows the solubility limit of Li atoms (lateral axis) as a function of the coherency factor α (vertical axis), which is obtained by solving $\partial(f + E_s)/\partial\phi = 0$ at each α. As the elastic effect becomes large, Li atoms become

more soluble; i.e., the miscibility gap decreases. Thus, the solubility of Li can be changed by the coherent elastic effect caused by the lattice mismatch.[6–8] In general, when the particle size is sufficiently large, misfit dislocations can be easily introduced, but when the particle size decreases, as a rule of thumb, they are inclined to be scarcely introduced into crystals. For this reason, it is considered that Li solubility increases with a decrease in particle size. However, it should be noted that the miscibility gap is not, in principle, absent, even with the complete coherent interface. If the (100) interface (i.e., the *bc* plane) cannot be formed for some reason, the miscibility gap would disappear, but it is difficult to assume such a case from the discussion above. Thus, we can conclude that there is a lower limit of the coherent misfit effects on the miscibility gap.

3.2. Effects of interfacial energy

The interfacial energy is frequently discussed as another cause of the increase in Li-solubility when the particle size becomes small. As described in Ref. [15], the interfacial energy γ as a function of ϕ can be approximately expressed as $\gamma \approx \gamma_{\mathrm{e}}(1-2\phi)^2$. Based on the literature,[13, 14] the interfacial energy γ_{e} can then be expected to be in the range from 40 to 100 mJ/m^2, and we can evaluate the effect of the interfacial energy on particle size by assuming that one interface is formed in the middle of a perpendicular-parallelepiped particle.

Figure 2(c) shows the sum of the chemical free energy given by Eq. (1) and interfacial energy per unit volume, i.e. $\left(f(\phi)SL+\gamma(\phi)S\right)/SL = f(\phi)+\gamma(\phi)/L$, as a function of ϕ and L, where L denotes a dimension of the particle that is normal to the interface S. Although the interfacial energy affects the Li solubility of small particles, we find that the effect is not so large unless a dimension L is extremely small (less than about 3 nm for $\gamma_{\mathrm{e}} = 100$ mJ/m^2 and there is virtually little effect for $\gamma_{\mathrm{e}} = 40$ mJ/m^2). Thus, it is shown that the single-phase reaction observed for particle diameter of 10-40 nm cannot be explained based on consideration of only interfacial energy.

3.3. Effects of both energies

In light of the previous experimental findings regarding the Li solubility in sub-micrometer-sized particles,[6–8] we cannot consider the elastic strain effect as a primary cause, since the elastic effect would be greater than the interface effect in such relatively large size and is always possible to yield a change in Li solubility regardless of the particle size. Hence, it would be vitally important to consider the effects of elastic strain on nano-sized particles in addition to the interface energy. Figure 2(d) shows the total free energy (including the elastic strain and interfacial energies) as a function of ϕ and L, where the (100) interface is assumed for the calculation. In this case, it is indicated that the single-phase reaction can take place when the particle size is under 4 nm for $\gamma_{\mathrm{e}} = 40$ mJ/m^2 and 10 nm for $\gamma_{\mathrm{e}} = 100$ mJ/m^2. The estimated size for the single-phase reaction is close to the actual observations but is still rather smaller than the experimental values (about 10-40 nm). These estimated values are considered as the limits of static thermodynamic in an infinite time scale. We would need to consider the single-phase reaction on the basis of the kinetics viewpoint in order to understand the actual finite-time-scale phase-separation process.

4. PREFERRED WAVELENGTH FOR SPINODAL DECOMPOSITION AND THE CRITICAL SIZE FOR NUCLEATION

Generally, the preferred wavelength of spinodal decomposition and the critical nucleation size are greatly affected by the elastic strain energy that accompanies transformations. According to the Cahn-Hilliard theory,[16–18] a critical or preferred wavelength is very important for the actual spinodal decomposition process in the time evolution of the spinodal wave. In the initial stage of decomposition, a linear approximation of the one-dimensional Cahn equation can be given by

$$\frac{\partial \phi}{\partial t} \approx M\Big(\frac{\partial^2 f_{\mathrm{tot}}}{\partial \phi^2}\Big)_{\phi_0}\frac{\partial^2 \phi}{\partial x^2} - 2MK_{\mathrm{S}}\frac{\partial^4 \phi}{\partial x^4}, \tag{3}$$

where M is the kinetic coefficient, K_{S} is the gradient energy, and f_{tot} is the sum of the chemical free energy function and the elastic strain energy function. The solution of this differential equation is simply expressed as $\phi(x,t) \approx \phi_0 + A(k,0)\exp[R(k)t]\exp(ikx)$, where A is a constant, k is the wavenumber, and $R(k)$ is called the concentration

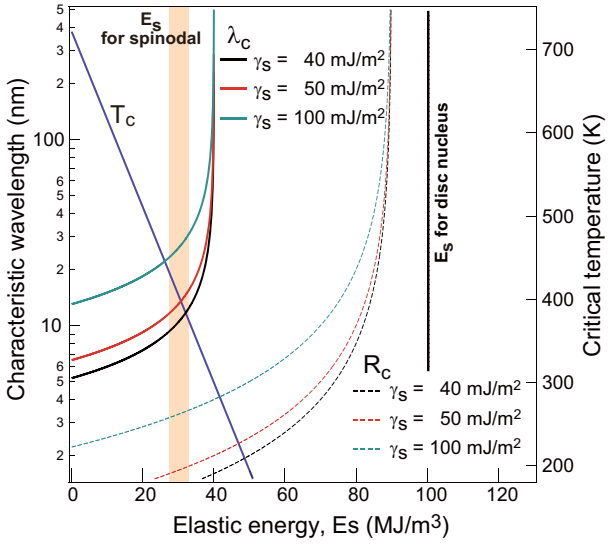

FIG. 3: The preferred wavelength λ_c and critical radius R_c in spinodal decomposition and nucleation processes in the $LiFePO_4/FePO_4$ system at 300 K, respectively. These values are estimated for three gradient coefficients $K_S \approx 0.5\times10^{-10}$, 0.9×10^{-10}, and 3.5×10^{-10} J/m, which correspond to the interfacial energies $\gamma_S = 40, 50$, and 100 mJ/m^2, respectively.

amplification factor and is expressed as

$$R(k) = -M\left(\frac{\partial^2 f_{\rm tot}}{\partial\phi^2}\right)_{\phi_0} k^2 - 2MK_{\rm S}k^4, \tag{4}$$

where $R(k) > 0$ is required for stable growth of the spinodal wave. Note that the case of $k = 0$ corresponds to the thermodynamic limit mentioned above, and a concentration wave with such a long wavelength cannot grow stably or grow at a quite slow rate from the kinetics viewpoint (because $R(k) \approx 0$).

From this condition, the preferred wavelength λ_c ($\equiv 2\pi/k_c$) of spinodal decomposition, at which the rate of spinodal decomposition is the greatest, is given by

$$\lambda_c \approx 2\pi\sqrt{\frac{2K_{\rm S}}{\Omega - 4E_{\rm s} - 2RT}}, \tag{5}$$

where E_s used here is the magnitude of Eq. (2) at $\phi = 1$. Incidentally, the critical wavelength that gives $R(k) = 0$ is $\lambda_c/\sqrt{2}$, but we should actually discuss the phase decomposition using the preferred wavelength as well as the above discussion. The critical temperature T_c is defined as the temperature where the magnitude of λ_c diverges to infinity; T_c is expressed as $T_c \approx (\Omega - 4E_s)/2R$.

Figure 3 shows the preferred wavelength of spinodal decomposition, λ_c, the critical nucleation radius, R_c for various interfacial energies (γ_S), and T_c as a function of the elastic strain energy E_s for the $LiFePO_4$ system. An elastic strain energy E_s of about 40 MJ/m^3 leads to divergence of the preferred wavelength λ_c for spinodal decomposition. As discussed above, E_s for spinodal decomposition is approximately 30 MJ/m^3 in this system (yellow-colored region), where λ_c is about 10-30 nm for $K_S \approx 0.5$-3.5×10^{-10} J/m. This value corresponds to $\gamma_S \approx \sqrt{K_S\Delta f_{\rm max}} \approx$ 40-100 mJ/m^2, where $\Delta f_{\rm max}$ is the free-energy difference between $\phi = 0.5$ and $\phi = \phi_e$ (equilibrium order parameter). Spinodal decomposition would be significantly suppressed when the particle size is less than these values, which well explains the present experimental result that the single-phase reaction took place for nano-sized particles of about 10 nm as shown in Fig. 1(c). Furthermore, the critical temperature T_c decreases significantly from about 720 K to about 400 K due to the elastic effect without any lattice mismatch. Thus, the driving force of spinodal decomposition is decreased at room temperature from this viewpoint on T_c.

Finally, we consider the case of nucleation. As shown in Fig. 3, E_s of about 90 MJ/m^3 yields divergence of the critical radius R_c for nucleation, since the driving force of nucleation is about 90 MJ/m^3 according to our previous paper.[15] In the paper, we calculated the elastic strain energy for the formation of an infinitesimal $FePO_4$ nucleus in the infinite homogeneous $LiFePO_4$ matrix, and showed that the minimum value of E_s is about 100 MJ/m^3. Thus, the elastic strain energy in the case of completely coherent formation is beyond the chemical driving force, i.e.,

$\Delta f_{\rm chem} + E_{\rm s} > 0$, which hinders the nucleation of $FePO_4$ in the $LiFePO_4$ matrix under charging ($LiFePO_4$ formation in the $FePO_4$ matrix on discharge).

5. CONCLUSIONS AND REMARKS

In conclusion, we have addressed the effects of elastic strain due to a lattice mismatch and gradient (interfacial) energy on the phase-separation behavior of olivine $LiFePO_4$, and have revealed experimentally and theoretically the mechanism of single-phase delithiation/lithiation reactions that has hitherto been unclear. We have shown experimentally that nano-sized particles (about 10 nm in diameter) did not show phase separation and were charged in a single phase state for the first time. In addition, we clarified the mysterious phenomenon of why the single-phase reaction proceeds with very small particles. In general, the specific surface area of particles increases with a decrease in particle size. Thereby, the elastic strain is believed to be easily released in smaller particles, and the phase separation is thought to be facilitated; however, actually, this is not the case. The present experiments have revealed that nano-sized particles tend to undergo a single-phase reaction. If we only consider this phenomenon from the viewpoint of static thermodynamics, the single-phase reaction cannot be explained unless the particle size is extremely small (below 4-10 nm). It is important to consider the phenomenon from a kinetic viewpoint, i.e., we must consider whether a single-phase reaction or phase separation takes place based on the concept of a preferred wavelength of spinodal decomposition. We should emphasize that extremely small nanoparticles would not undergo phase separation in terms of kinetics, and a certain appropriate particle size (more than about 10-30 nm in this case) is required for the phase separation.

In our previous paper[15], the initial condition associated with the gradient term of the Li concentration was considered by using the numerical simulation based on the Cahn-Hilliard equation. Our simulation suggested that, in such a case, a domain wall motion like domino cascade[26] can surely occur, but the spinodal decomposition is still dominant even in the case. Thus, the gradient term tends to promote the domain wall motion, but this motion is very sluggish because of the strain energy effect. Actually, in our experiment, the phase separation cannot take place in very small nanoparticles, which indicates that the gradient term plays just a role in the macroscopic change of the Li concentration in the bulk. Thus, the fact that the single-phase reaction occurs without the phase separation strongly indicates that the charge/discharge process of $LiFePO_4$ cannot be explained only by the domino cascade model, but the phase separation as a transformation is also inevitably involved in the charge/discharge process of normal sized particles.

Acknowledgements

The authors wish to thank Yosuke Yamada and Kuniko Chihara in Kyushu University for their help with the TEM observation and charge/discharge measurements.

[1] A. K. Padhi, K. S. Nanjundaswamym, J. B. Goodenough, *J. Electrochem. Soc.*, 1997, **144**, 1188-1194.
[2] H. Huang, S. C. Yin, L. F. Nazar, *Electrochem. Solid-State Lett.*, 2001, **4**, A170-A172.
[3] S. Y. Chung, J. Bloking, Y. M. Chiang, *Nat. Mater.*, 2002, **1**, 123-128.
[4] A. Yamada, S. C. Chung, K. Hinokuma, *J. Electrochem. Soc.*, 2001, **148**, A224-A229.
[5] A. Yamada, H. Koizumi, S. Nishimura, N. Sonoyama, R. Kanno, M. Onemura, T. Nakamura, & Y. Kobayashi, *Nat. Mater.*, 2006, **5**, 357-360.
[6] N. Meethong, H.-Y. S. Huang, W. C. Carter, Y.-M. Chiang, *Electrochem. Solid-State Lett.*, 2007, **10**, A134-A138.
[7] G. Kobayashi, S. Nishimura, M.-S. Park, R. Kanno, M. Yashima, T. Ida, A. Yamada, *Adv. Funct. Mater.*, 2009, **19**, 395-403.
[8] N. Meethong, H.-Y. S. Huang, S. A. Speakman, W. C. Carter, Y.-M. Chiang, *Adv. Funct. Mater.*, 2007, **17**, 1115-1123.
[9] P. Gibot, M. Casas-Cabanas, L. Laffont, S. Levasseur, P. Carlach, S. Hamelet, J.-M. Tarascon, C. Masquelier, *Nat. Mater.*, 2008, **7**, 741-747.
[10] H.-H. Chang, C.-C. Chang, H.-C. Wu, M.-H. Yang, H.-S. Sheu, N.-L. Wu, *Electrochem. Commun.*, 2008, **10**, 335-339.
[11] J. B. Leriche, S. Hamelet, J. Shu, M. Morcrette, C. Masquelier, G. Ouvrard, M. Zerrouki, P. Soudan, S. Belin, E. Elkaïm, F. Baudelet, *J. Electrochem. Soc.*, 2010, **157**, A606-A610.
[12] X. J. Wang, C Jaye, K. -W. Nam, B. Zhang, H. -Y. Chen, J. Bai, H. Li, X. Huang, D. A. Fischer, X. -Q. Yang, *J. Mater. Chem.*, 2011, **21**, 11406-11411.
[13] M. Wagemaker, F. M. Mulder, A. Van der Ven, *Adv. Mater.*, 2009, **21**, 2703-2709.
[14] D. A. Cogswell, M. Z. Bazant, *ACS Nano*, 2012, **6**, 2215-2225.
[15] T. Ichitsubo, K. Tokuda, S. Yagi, M. Kawamori, T. Kawaguchi, T. Doi, M. Oishi, E. Matsubara, *J. Mater. Chem. A*, 2013, **1**, 2567-2577.
[16] J. W. Cahn, J. E. Hilliard, *J. Chem. Phys.*, 1958, **28**, 258-267.
[17] J. W. Cahn, *Acta Metall.*, 1961, **9**, 795-801.
[18] J. W. Cahn, *Acta Metall.*, 1962, **10**, 179-183.
[19] T. Doi, S. Yatomi, T. Kida, S. Okada, J. Yamaki, *Cryst. Growth Des.*, 2009, **9**, 4990-4992.
[20] M. Tang, J. F. Belak, M. R. Dorr, *J. Phys. Chem. C*, 2011, **115**, 4922-4926.
[21] R. Malik, F. Zhou, G. Ceder, *Nat. Mater.*, 2011, **10**, 587-590.
[22] W. Dreyer, J. Jamnik, C. Guhlke, R. Huth, J. Moškon, M. Gaberščcek, *Nat. Mater.*, 2010, **9**, 448-453.
[23] C. V. Ramana, A. Mauger, F. Gendron, C. M. Julien, K. Zaghib, *J. Power Sources*, 2009, **187**, 555-564.
[24] T. Maxisch, G. Ceder, *Phys. Rev. B*, 2006, **73**, 174112.
[25] G. Chen, X. Song, T. J. Richardson, *Electrochem. Solid-State Lett.*, 2006, **9**, A295-A298.
[26] C. Delmas, M. Maccario, L. Croguennec, F. Le Cras, F. Weill, *Nat. Mater.*, 2008, **7**, 665-671.